Conformational Properties of Substituted Ferrocenes: Experimental and Theoretical Studies of the Molecular Structures of 1,1′-Di-*tert*-butylferrocene and Isopropylferrocene

Carole A. Morrison, Simon F. Bone, David W. H. Rankin, Heather E. Robertson, Simon Parsons, Robert A. Coxall, and Stewart Fraser

Department of Chemistry, University of Edinburgh, West Mains Road, Edinburgh, EH9 3JJ, United Kingdom

James A. S. Howell,* Paul C. Yates, and Natalie Fey

Lennard-Jones Laboratories, School of Chemistry and Physics, Keele University, Staffordshire ST5 5BG, United Kingdom

Received November 27, 2000

The molecular structures of 1,1′-di-*tert*-butylferrocene (**1**) and isopropylferrocene (**2**) have been examined by solid-state X-ray crystallography, gas-phase electron diffraction, and DFT and molecular mechanics calculations. Whereas the solid-state structure of **1** has crystallographically imposed staggered C_{2h} symmetry, electron diffraction and calculations support a mixture of C_2 eclipsed isomers. The eclipsed ring−ring and the ring−isopropyl conformations found for **2** are essentially identical in the solid and gas phase and are supported by calculations. The molecular mechanics analysis may be extended to other alkylferrocene derivatives.

Introduction

Ferrocenyl compounds continue to attract considerable research interest, being used in areas as diverse as homogeneous metal-catalyzed organic synthesis,[1a−c] as advanced materials with compounds possessing novel conducting, magnetic, or optical properties,[2a−d] and as the redox active component in a variety of host−guest systems with potential application as novel sensors.[3a−d]

Particularly in the case of catalysis, an understanding of molecular structure and conformation is important in rational ligand design. Assessing the molecular structure of simple ferrocene complexes can, however, present problems for all current structural methods. For example, in the solid state, crystal packing effects may easily impose higher molecular symmetry as the energy barrier to ring reorientation is so small (5−14 kJ mol^{-1} for the monoclinic and triclinic forms of ferrocene itself).[4a,b] Although more information concerning the conformational properties can be gleaned in the gas phase by electron diffraction, the presence of many similar distances may result in only a partial structure being obtained. For theory, accurate calculation of equilibrium structures of transition metal complexes using the standard techniques of ab initio quantum mechanics can be notoriously difficult, with the Fe−X (X = center of cyclopentadienyl ring) distance in ferrocene being a prime example of a parameter that varies widely with the computational method. Finally, for molecular mechanics, in contrast to the organic literature, there still remain relatively few reports of force fields for organometallic compounds, including ferrocenes.[5a,b] This may be attributed in part to a lack of suitable parametrization and in part to the ambiguity in the structural representation of metal−hydrocarbon π-complexes, although in general the use of realistic bonding models is not a requirement of molecular mechanics.

Thus, an integrated approach in which different techniques contribute to an overall understanding of structure seems particularly appropriate for ferrocenyl compounds.[6] The Fe−X distance will be extremely well determined by electron diffraction and is the hardest parameter to calculate reliably ab initio. The gas-phase experimental structure can therefore be used to assess the performance of the calculations. In turn, the calcu-

* Corresponding author. Fax: +44 1782 712378. E-mail: jashowell@chem.keele.ac.uk.

(1) (a) Richards, C. J.; Locke, A. J. *Tetrahedron: Asymmetry* **1998**, *9*, 2377. (b) Dai, L.; Hou, X.; Deng, W.; You, S.; Zhou, Y. *Pure Appl. Chem*. **1999**, *71*, 1401. (c) Togni, A.; Bieler, N.; Burckhardt, U.; Kollner, C.; Pioda, G.; Schneider, R.; Schnyder, A. *Pure Appl. Chem*. **1999**, *71*, 1531.

(2) (a) Whittall, I. R.; McDonagh, A. M.; Humphrey, M. G. *Adv. Organomet. Chem*. **1999**, *43*, 349. (b) Nguyen, P.; Gomez-Elipe, P.; Manners, I. *Chem. Rev*. **1999**, *99*, 1515. (c) Barlow, S.; O'Hare, D. *Chem. Rev*. **1997**, *97*, 637. (d) Cuadrado, I.; Moran, M.; Casado, C. M.; Alonso, B.; Losada, J. *Coord. Chem. Rev*. **1999**, *193*−*95*, 395. (e) Barlow, S.; Marder, S. R. *Chem. Commun*. **2000**, 1555.

(3) (a) Kaifer, A. E. *Acc. Chem. Res*. **1999**, *32*, 62. (b) Cardona, C. M.; Mendoza, S.; Kaifer, A. E. *Chem. Soc. Rev*. **2000**, *29*, 37. (c) Beer, P. D. *Acc. Chem. Res*. **1998**, *31*, 71. (d) Beer, P. D.; Gale, P. A.; Chen, Z. *Adv. Phys. Org. Chem*. **1998,** *31*, 1.

(4) (a) Braga, D. *Chem. Rev*. **1992**, *92*, 633. (b) Dunitz, J. D. *Acta Crystallogr*. **1995**, *B51*, 619. (c) Seiler, P.; Dunitz, J. D. *Acta Crystallogr*. **1982**, *B38*, 1741.

(5) For an overview of other molecular mechanics approaches, see: (a) Fey, N. *J. Chem. Technol. Biotechnol*. **1999**, *74*, 852. (b) Comba, P.; Gyr, T. *Eur. J. Inorg. Chem*. **1999**, 1787.

(6) Ebsworth, E. A. V.; Rankin, D. W. H.; Cradock, S. *Structural Methods in Inorganic Chemistry*; Blackwell Scientific Publications: Oxford, 1987; Chapter 10.

10.1021/om001012w CCC: $20.00
Publication on Web 05/01/2001

Table 1. Structural and Thermodynamic Parameters for Ferrocene

parameter[a]	MM[b]	DFT[b]	GED[c]	XRD[d]
*r*Fe−X	1.66	1.658	1.661(4)	av 1.653
*r*Fe−C_{ring}	2.09	2.051	2.064(3)	av 2.055
*r*C−C	1.44	1.427	1.440(2)	av 1.435
*r*C−H	1.08	1.082		
∠Fe−C−H	128.1	125.2		av 126.4
tw ring	0.0	0.0	0.0	0.0
Δ*E*(staggered − eclipsed)	4.3	3.4	4(1)	

[a] Abbreviations used: *r* = bond distance/Å, ∠ = angle/deg, tw = twist/deg, X = center of cyclopentadienyl ring, Δ = enthalpy difference in kJ mol^{-1}. [b] This work, see text for details. [c] Ref 8. [d] Ref 4c.

lations generate reliable energies for the different conformational minima, which can then be used to assess the quality of the molecular mechanics force field. This force field can then be used to easily examine the whole conformational energy surface. Any difference in molecular geometry induced by a change in phase can then be assessed by comparison with the solid-state structures.

In this paper we report the gas- and solid-phase structures of 1,1′-di-*tert*-butylferrocene (**1**) and isopropylferrocene (**2**) determined by gas-phase electron diffraction, X-ray crystallography, and density functional theory, together with a molecular mechanics analysis of their conformational isomerism, which may be extended to similar compounds. Compound **2** was chosen as a simple example of rotational isomerism about a ring−carbon bond containing a saturated substituent, while **1** exemplifies inter-ring conformational isomerism in a sterically demanding 1,1′-disubstituted derivative.

Results and Discussion

Calculating reliable geometries for transition metal complexes using standard ab initio methods can be quite difficult. The Hartree−Fock level, in neglecting the all-important effects of electron correlation, overestimates the Fe−X distance in ferrocene by over 20 pm, whereas the MP2 method overestimates the correlation effect and generates a distance short by 20 pm.[7a] Considerable success was recently achieved at the CCSD(T) level with a substantial basis set and including all electrons in the correlation.[7b] However, such computationally demanding calculations require hardware resources out of reach of most research groups. The application of the less computationally demanding density functional theory (DFT) to ferrocenes, however, has been remarkably successful in reproducing experimental rotational barriers and ground-state geometries.[7c−f] For this work, we have found that the use of conventional 6-31G* basis sets for carbon and hydrogen and Wachters+f for iron with the DFT hybrid functional B3PW91 gave excellent agreement with the experimental geometry of ferrocene on a modest-sized workstation (Table 1). The calculation also correctly identifies the eclipsed structure as the energy minimum and gives a rotational barrier of 3.4 kJ mol^{-1}, close to the experimental value.[8]

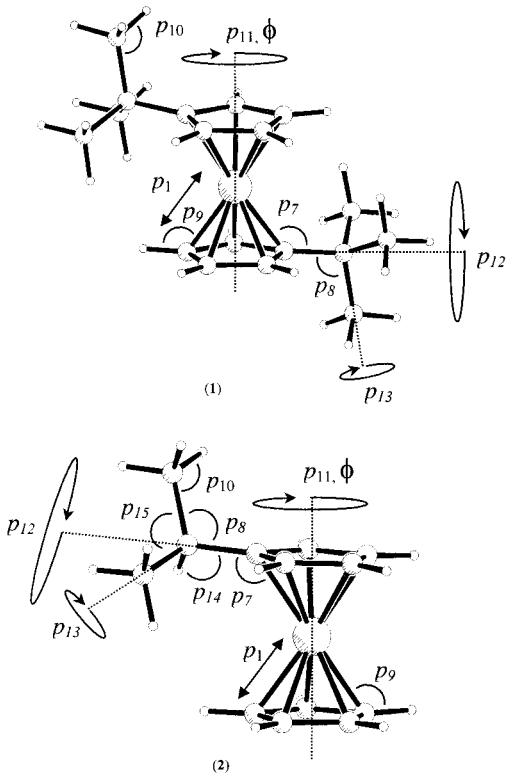

Figure 1. Molecular structures of **1** and **2**; labels define parameter sets used in GED refinements.

For the molecular mechanics work, a dummy atom approach[9a,b] was adapted using HyperChem,[10] in which all forces were redistributed among the defining atoms by continual recalculation. The dummy atoms were defined as a new atom type LP1 (mass = 0.001 g mol^{-1}, radius = 0.001 Å), and positions were determined by tethering each to a POINT defined as the center of mass of the surrounding cyclopentadienyl carbons, with a high force constant (500 kcal mol^{-1} Å^{-2}). A script of commands redefined the POINT position after five iterations, which was found sufficient to account for any movement of the defining cyclopentadienyl carbons. The script also permitted alternation between the two rings after a set number of cycles until the required convergence gradient had been achieved for both rings. Dummy atoms were held in the ring plane by assignment of ideal zero degree values and a high force constant (500 kcal mol^{-1} deg^{-2}) to the improper torsions shown in Figure 2. At the end of an optimization, all computational restraints were removed and a single-point energy was calculated for this geometry. As no direct carbon−dummy bonds are present, this approach does not require additional torsional parameters to describe interactions between the dummy atoms and the cyclopentadienyl carbons. Original MM+ parameters were used with a few additions or modifications (see Experimental Section). The high force constant for the LP1-Fe term was required to overcome the tendency of the rings to move apart. Equilibrium values for some of the purely organic terms were adjusted to represent idealized ferrocene geometry, while retaining the original force constants.

(7) (a) Klopper, W.; Lüthi, H. P. *Chem. Phys. Lett.* **1996**, *26*, 35. (b) Koch, H.; Jorgenson, P. *J. Chem. Phys.* **1996**, *104*, 9528. (c) Berces, A.; Ziegler, T. *Top. Curr. Chem.* **1996**, *182*, 41. (d) Berces, A.; Ziegler, T.; Fan, L. *J. Phys. Chem.* **1994**, *98*, 1584. (e) Hohm, U.; Goebel, D.; Grimme, S. *Chem. Phys. Lett.* **1997**, *272*, 328. (f) Mayor-Lopez, M. J.; Weber, J. *Chem. Phys. Lett.* **1997**, *281*, 226.

(8) Haaland, A.; Nilsson, J. *Acta Chem. Scand.* **1968**, *22*, 2653.

(9) (a) Thompson, N. D.; Landis, C. R.; Bosnich, B. *J. Am. Chem. Soc.* **1992**, *114*, 7264. (b) Bosnich, B. *Chem. Soc. Rev.* **1994**, *23*, 387.

(10) *HyperChem 5.11*; Hypercube Inc.: Gainesville, FL 32601, 1996.

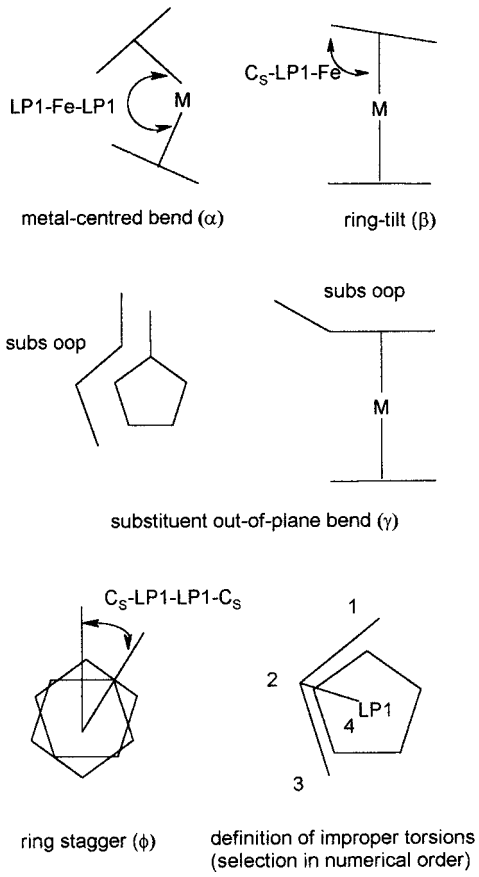

Figure 2. Definition of geometric parameters used in molecular mechanics minimizations.

Simulation of the 5-fold rotational barrier for ferrocene is not possible using the V_1, V_2, and V_3 torsional parameters available in HyperChem. Since it has been shown that the only contribution of a V_5 term is to the torsional energy,[9a] a correction corresponding to a rotational barrier of 1 kcal mol^{-1} in favor of the eclipsed conformation was added to the calculated energies using the torsional energy expression $E_t = 0.5V_5[1 + \cos(5\phi)]$, where ϕ represents the inter-ring torsional angle and $V_5 = -1$ kcal mol^{-1}.

The force field reproduces well the structure of ferrocene as determined by gas-phase electron diffraction (Table 1) and was further tested in the simulation of the strained ferrocenophanes[11a,b] **3**−**6**. In general, the agreement with data obtained from single-crystal structure determinations[12a−c] was good (Table 2) and the force field showed sufficient versatility to include relaxation of the structure through metal-centered bending, ring tilting, and substituent out-of-plane bending as defined in Figure 2.

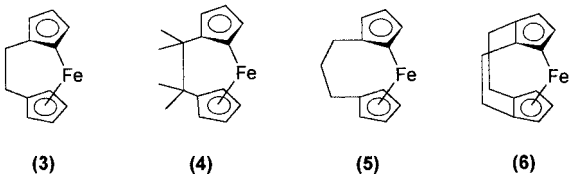

A. Molecular Structure of 1,1′-Di-*tert*-butylferrocene (1). Crystals suitable for X-ray analysis were obtained by slow cooling to 20 °C in a glass capillary.

Table 2. Comparison of Experimental and Modeled Structures for 3−6[a]

	experimental	modeled
	3	
C_S-Fe	1.97 Å	1.99 Å
LP1−Fe	1.63 Å	1.66 Å
α	164°	165°
β	−3.7°	−4.6°
γ	20° toward Fe	15.3° toward Fe
ϕ	1.2°	11.8 °
	4	
C_S−Fe	1.97 Å	1.99 Å
LP1−Fe	1.65 Å	1.66 Å
α	160°	164°
β	−3.6°	−4.8°
γ	14.5° toward Fe	12.2° toward Fe
ϕ	9.2°	11.5°
	5	
C_S−Fe	2.02 Å	2.04 Å
LP1−Fe	1.63 Å	1.66 Å
α	174°	173°
β	−0.8°	−1.4°
γ	7.8° toward Fe	4.1° toward Fe
ϕ	0.1°	0.1°
	6	
C_S−Fe	2.02 Å	2.04 Å
LP1−Fe	1.63 Å	1.66 Å
α	170°	172°
β	−1.3°	−1.5°
γ	4.5° toward Fe	3.6° toward Fe
ϕ	1.1°	0.5°

[a] C_S refers to the substituted carbon atoms. Geometric parameters α, β, γ, ϕ as defined in Figure 2, again referring to the substituted carbon atom.

The molecular geometry obtained (Figure 3a) has parallel cyclopentadienyl rings with the *tert*-butyl groups bent out of the plane and away from the iron by 6.0°. The molecule has an inversion center imposed crystallographically by the $P\bar{1}$ space group. However, this conformation may well not represent the gas-phase or solution molecular energy minimum, as the barrier to internal ring rotation is expected to be quite low. Of the 33 crystal structures for unbridged symmetrically substituted 1,1′-ferrocenes with achiral substituents retrieved from the Cambridge Crystallographic Data Base[13] (Table 3), nearly half also have C_{2h} symmetry (i.e., ring torsion $\phi = 180°$) imposed crystallographically. Six possess a nearly eclipsed conformation ($\phi < 10°$) with hydrogen-bond interactions important in three of these cases to maintain the eclipsed structure. The remaining structures fall generally into two groups with the ring torsional angle ϕ in the range 50−80° or 119−150°. Uniquely, 1,1′-diformylferrocene has one molecule of each type in the solid-state lattice.

Examination of the molecular mechanics energy profile obtained for ring rotation in **1** (Figure 4) shows two minima at 72° and 144° (Figure 3b), with the former being slightly lower in energy by 1.1 kJ mol^{-1}. A Boltzmann analysis at 293 K provides a relative population ratio of 1.0:0.9 and a predicted weighted ring

(11) For reviews, see: (a) Heo, R. W.; Lee, T. R. *J. Organomet. Chem.* **1999**, *578*, 31. (b) Green, J. C. *Chem. Soc. Rev.* **1998**, *27*, 263.
(12) (a) Nelson, J. M.; Rengel, H.; Petersen, R.; Nguyen, P.; Lough, A. J.; Manners, I. M.; Aju, N. P. R.; Greedan, J. E.; Barlow, S.; O'Hare, D.; McDonald, P. M. *Chem.−Eur. J.* **1997**, *3*, 573. (b) Lain, M. B.; Trueblood, K. N. *Acta Crystallogr.* **1965**, *19*, 373. (c) Hillman, M.; Austin, J. D. *Organometallics* **1987**, *6*, 1737.
(13) Fletcher, D. A.; McMeeking, R. F.; Parkin, D. *J. Chem. Inf. Comput. Sci.* **1996**, *36*, 746.

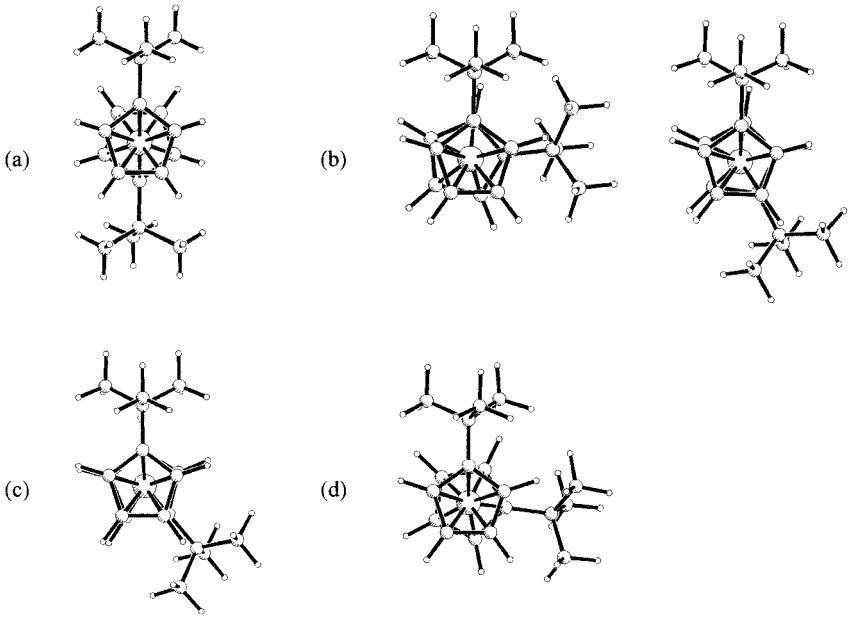

Figure 3. Molecular structures of **1**: (a) X-ray diffraction, (b) molecular mechanics global and local minima ($\phi = 72°$ and 144°, respectively), (c) DFT minimum, and (d) gas-phase electron diffraction.

torsion value (ϕ, p_{11}) of 106°. The molecular mechanics torsional energy profile rises steeply below 72°, reaching a maximum at the 0° eclipsed configuration, where significant metal−ring bending and ring−substituent bending are required to relieve substituent−substituent interactions. The fluxionality of **1** may thus be viewed as a large-amplitude oscillation of low energy between 72⟨180⟩-72°, via barriers of 3 and 10 kJ mol^{-1} at 108° and 180°, respectively, coupled with a higher energy passage of the *tert*-butyl groups past one another (35 kJ mol^{-1}). The solid-state barrier to ring rotation in **1** has been estimated at 28.4 kJ mol^{-1}.[15] The value of the *tert*-butyl twist parameter p_{12} predicted by molecular mechanics was very similar for both energy minima (av 178.3°). Examination of the energy profile for ring−*tert*-butyl rotation shows that the two substituents rotate independently of one another at both energy minima with a 3-fold barrier of 6.0 kJ mol^{-1}, compared to 14.6 kJ mol^{-1} estimated in the solid state.[15]

In view of the results obtained by molecular mechanics, the conformational potential energy surface of **1** was probed by DFT using the same level of calculation as for ferrocene, with a starting value for the ring torsional angle ϕ of 180°. An energy minimum with overall C_2 symmetry (Figure 3c, Table 4) was found nearby ($\phi =$ 140.2°). Information concerning the curvature of the potential energy surface at this minimum was obtained from the calculated vibrational frequencies. The ring torsional mode corresponding to the lowest vibrational frequency (just 21 cm^{-1}) indicates that the potential energy surface at this point must be very flat. The next two lowest frequencies calculated at ca. 58 and 60 cm^{-1} correspond to the symmetric (A) and asymmetric (B) modes of the *tert*-butyl torsional motion (p_{12}).

The experimental gas-phase structure for **1** was then obtained by simulating the electron diffraction data set using a mathematical model that describes the molecular geometry in terms of a set of refinable parameters (see Experimental Section). Using both experimental GED data and values from DFT calculation for p_5 and p_6, a full structure solution was obtained using the SARACEN method[16] (Table 4). In general, the parameters defining the key features on the radial distribution

(14) (a) Wrackmeyer, B.; Dorfler, U.; Milius, W.; Herberhold, M. *Polyhedron* **1995**, *14*, 1425. (b) Pilloni, G.; Corain, B.; Degano, M.; Longato, B.; Zanotti, G. *J. Chem. Soc., Dalton Trans.* **1993**, 1777. (c) Larre, C.; Donnadieu, B.; Caminade, A. M.; Majoral, J. P. *Eur. J. Inorg. Chem.* **1999**, 601. (d) Schottenberger, H.; Buchmeiser, M.; Rieker, C.; Jaitner, P.; Wurst, K. *J. Organomet. Chem.* **1997**, *541*, 249. (e) Byrne, J. J.; Rebello, A.; Chavant, P. A.; Averbuch-Pouchot, M. T.; Vallee, Y. *Z. Kristallogr.-New Cryst. Struct.* **1998**, *213*, 180. (f) Casellato, U.; Ajo, D.; Valle, G.; Corain, B.; Longato, B.; Graziani, R. *J. Cryst. Spectrosc. Res.* **1988**, *18*, 583. (g) Foucher, D. A.; Honeyman, C. H.; Lough, A. J.; Manners, I.; Nelson, J. M. *Acta Crystallogr.* **1995**, *C51*, 1795. (h) Adeleke, J. A.; Chen, Y. W.; Liu, L. K. *Organometallics* **1992**, *11*, 2543. (i) Szulzewsky, K.; Seidel, I.; Kulpe, S.; Hohne, E.; Raubach, H.; Stoffer, U. *Krist. Tech.* **1979**, *14*, 37. (j) Yamamoto, Y.; Tanase, T.; Mori, I.; Nakamura, Y. *J. Chem. Soc., Dalton Trans.* **1994**, 3191. (k) Fang, Z. G.; Hor, T. S. A.; Wen, Y. S.; Liu, L. K.; Mak, T. C. W. *Polyhedron* **1995**, *14*, 2403. (l) Pilloni, G.; Longato, B.; Bandoli, G.; Corain, B. *J. Chem. Soc., Dalton Trans.* **1997**, 819. (m) Benyei, A. C.; Glidewell, C.; Lightfoot, P.; Royles, B. J. L.; Smith, D. M. *J. Organomet. Chem.* **1997**, *539*, 177. (n) Palenik, G. J. *Inorg. Chem.* **1969**, *8*, 2744. (o) Takusagawa, F.; Koetzle, T. F. *Acta Crystallogr.* **1979**, *B35*, 2888. (p) Yuan, Y. F.; Ye, S. M.; Zhang, L. Y.; Wang, B.; Wang, J. T. *Polyhedron* **1997**, *16*, 1713. (q) Scott, P.; Rief, U.; Diebold, J.; Brintzinger, H. H. *Organometallics* **1993**, *12*, 3094. (r) Ingham, S. L.; Khan, M. S.; Lewis, J.; Lomg, N. J.; Raithby, P. R. *J. Organomet. Chem.* **1994**, *470*, 153. (s) Ferguson, G.; Gallagher, J. F.; Glidewell, C.; Zakaria, C. M. *Acta Crystallogr.* **1993**, *C49*, 967. (t) Butler, I. R.; Hobson, L. J.; Coles, S. J.; Hursthouse, M. B.; Abdul Malik, K. M. *J. Organomet. Chem.* **1997**, *540*, 27. (u) Carr, J. D.; Coles, S. J.; Hassan, W. W.; Hursthouse, M. B.; Abdul Malik, K. M.; Tucker, J. H. R. *J. Chem. Soc., Dalton Trans.* **1999**, 57. (v) Gimeno, C.; Jones, P. G.; Laguna, A.; Sarroca, C.; Calhorda, M. J.; Veiros, L. F. *Chem. Eur. J.* **1998**, *4*, 2308. (w) Seidelmann, O.; Beyer, L.; Zdobinsky, G.; Kirmse, R.; Dietze, F.; Richter, R. *Z. Anorg. Allg. Chem.* **1996**, *622*, 692. (x) Gallagher, J. F.; Ferguson, G.; Ahmed, S. Z.; Glidewell, C.; Lewis, A. *Acta Crystallogr.* **1997**, *C53*, 1772. (y) Palenik, G. J. *Inorg. Chem.* **1970**, *9*, 2424. (z) Kempe, R.; Spannenberg, A. *Z. Kristallogr.-New Cryst. Struct.* **1997**, *212*, 479. (aa) Hirotsu, K.; Higuchi, T.; Shimada, A. *Bull. Chem. Soc. Jpn.* **1968**, *41*, 1557. (bb) Grossel, M. C.; Goldspink, M. R.; Hriljac, J. A.; Weston, S. C. *Organometallics* **1991**, *10*, 851. (cc) Bradley, S.; McGowan, P. C.; Oughton, K. A.; Thornton-Pett, M.; Walsh, M. E. *Chem. Commun.* **1999**, 77. (dd) Singh, H. B.; Regini, A. V.; Jasinski, J. P.; Paight, E. S.; Butcher, R. J. *J. Organomet. Chem.* **1994**, *464*, 87. (ee) Braga, D.; Paganelli, F.; Tagliavini, E.; Casolari, S.; Cojazzi, G.; Grepioni, F. *Organometallics* **1999**, *18*, 4191. (ff) MacGillivray, L. R.; Spinney, H. A.; Reid, J. L.; Ripmeester, J. A. *J. Chem. Crystallogr.* **1999**, *29*, 865.

(15) Makova, M. K.; Leonova, E. V.; Karimov, Y. S.; Kochetkova, N. S. *J. Organomet. Chem.* **1973**,*55*, 185.

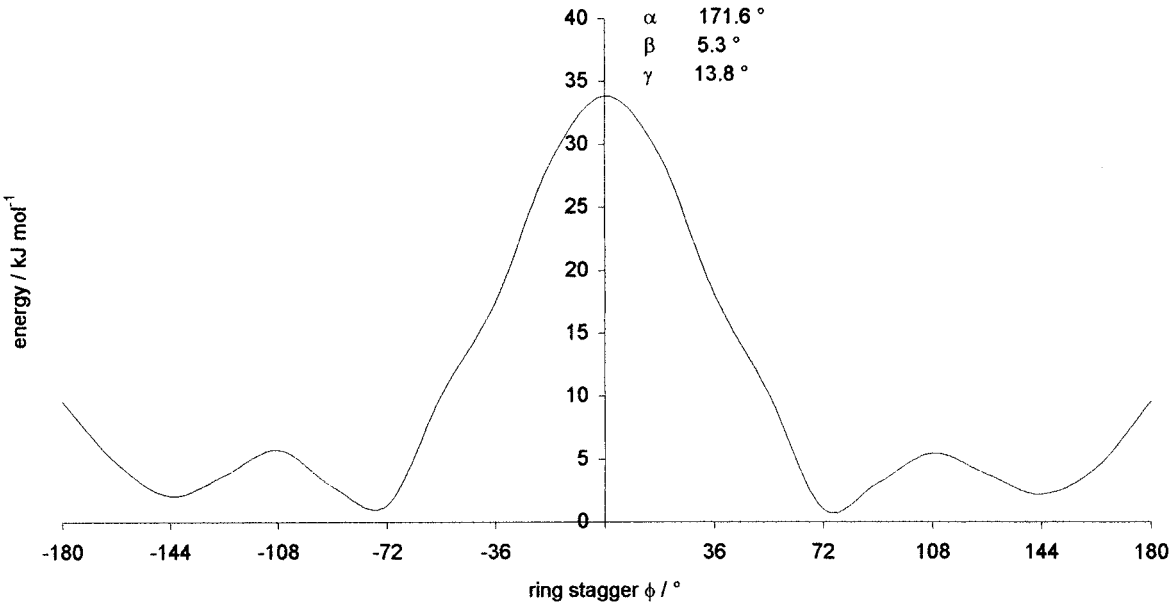

Figure 4. Ring rotation energy profile for **1**.

Table 3. Crystallographic Data for 1,1′-$(C_5H_4X)_2Fe$ Complexes

entry	X	space group (Z)	ϕ/deg	reference
1	^{t}Bu	$P\bar{1}$ (1)	180	this work
2−5	BBr_2, $P(O)Ph_2$, $Ph_2P{=}NP(O)(OPh)_2$, 7-hydroxynorborn-2-enyl	$P\bar{1}$ (1)	180	14a−d
6, 7	CH_2Ph, PPh_2	$P2_1/a$ (2)	180	14e,f
8−10	$SiMe_3$, SPh, C(O)(O)Ph	$P2_1/c$ (2)	180	14g−i
11	CH_2PPh_2	$P2_1/n$ (2)	180	14j
12, 13	$P(S)Ph_2$, $P(Se)Ph_2$	$C2/c$ (4)	180	14k,l
14	$C(O)C_6H_4OH$-*p*	*Pbcn* (4)	180	14m
15	COOH (monoclinic)	$P2_1/c$ (4)	2	14n
16	COOH (triclinic)	$P\bar{1}$(4)	1	14o
17	$C(O)NHC(S)NHC_6H_4Cl$-*p*	$P2_1/n$ (4)	9	14p
18	Me	$P2_1/c$ (4)	4	14a
19	3-indenyl	$C2/c$ (8)	8	14q
20	CCPh	$P2_1/c$ (4)	2	14r
21	$C(OH)Ph_2$	$C2/c$ (8)	51/56	14s
22	9-anthracenyl	$C2/c$ (8)	69	14t
23	$C(O)NHCH_2$(2-pyridyl)	$P\bar{1}$(2)	69	14u
24	$SC(S)NEt_2$	$P2_1/c$ (4)	76	14v
25	$C(O)NHC(S)NEt_2$	$P2_1/c$ (4)	85	14w
26	C(O)Ph	$P2_1/n$ (4)	119	14x
27	C(O)Me	$P2_1/c$ (4)	131	14y
28	$SiMe_2Cl$	$P\bar{1}$(2)	141	14z
29	Si_2Me_5	$P2_1/n$ (4)	143	14aa
30	C(O)NHMe	$C2/c$ (8)	140	14bb
31	4-(*N*-methylpiperidinyl)	$P\bar{1}$(2)	155	14cc
32	TePh	$P2_1/a$ (4)	170	14dd
33	C(O)H	$P2_1/n$ (8)	43/138	14ee, ff

curve (Figure 5) refined to values that agree well with the geometry calculated by DFT. The average C−H distance (p_3), giving rise to the first peak on the radial distribution curve, refined to 1.111(3) Å (1.088 Å calculated). The position of the second peak on the radial distribution curve is dictated by the average C−C distance (p_2), which refined to 1.481(1) Å, in exact agreement with the calculation. The third peak comprises three features. The first, at 2.069(1) Å, is attributed to the Fe−C_{ring} distance p_1 (calculated range 2.05−2.08 Å). The second feature at ca. 2.3 Å is assigned to $rC_{ring}\cdots C_{ring}$. As the cyclopentadienyl rings have assumed local C_{5v} symmetry, this distance will be defined purely by the C−C distance parameters p_2, p_4, and p_5. The third feature at ca. 2.5 Å is assigned to C···C distances involving the *tert*-butyl substituent and is therefore a function of the C−C distance parameters and the angles p_7 and p_8; both angles refined to acceptable values, with the value of p_7 indicating an out-of-plane bending away from the iron of 9.1° for the *tert*-butyl substituent. In the region to the right of the third peak is $r\text{Fe}\cdots H_{ring}$ (ca. 2.8 Å), which controls the value of p_9, Fe−C−H. This parameter, at 124.2(15)°, is within one esd of the calculated value and represents an out-of-plane bend of the ring C−H bonds toward the iron by 1.9°.

The remainder of the radial distribution curve dictates the overall conformation of the molecule in terms

(16) (a) Blake, A. J.; Brain, P. T.; McNab, H.; Miller, J.; Morrison, C. A.; Parsons, S.; Rankin, D. W. H.; Robertson, H. E.; Smart, B. A. *J. Phys. Chem.* **1996**, *100*, 12280. (b) Brain, P. T.; Morrison, C. A.; Parsons, S.; Rankin, D. W. H. *J. Chem. Soc., Dalton Trans.* **1996**, 4589.

Table 4. Structural Parameters Obtained for 1

	parameter[a]	XRD	MM[b] 72/144°	DFT[c]	GED[d]
	independent				
p_1	rFe−C_{ring}	av 2.06	av 2.09	2.05−2.08	2.069(1)
p_2	av rC−C	1.46	1.48	1.481	1.481(1)
p_3	av rC−H		1.10	1.088	1.111(3)
p_4	ΔrC−C_1			−0.102	−0.094(2)
p_5	ΔrC−C_2			−0.018(2)	−0.020(2)
p_6	ΔrC−H			−0.013(2)	−0.013(2)
p_7	∠Fe−C−C_{tBu}	132.7	132.6/130.7	133.6	131.6(3)
p_8	∠C_{ring}-C−C_{tBu}	av 110.5	av 110.1	av 110.1	112.3(3)
p_9	∠Fe−C−H		av 129.2	av 125.0	124.2(15)
p_{10}	∠C−C−H		av 111.5	av 111.0	109.6(11)
p_{11} (ϕ)	ring twist	180.0	72.3/143.8	140.2	97.7(4)
p_{12}	^{t}Bu twist	171.8	178.9/177.6	177.3	165.2(5)
p_{13}	Me twist		61.4/61.9	59.6	63(3)
	dependent				
	rFe−X	1.67	1.66	1.660	1.671(1)
	av $r$$C_{ring}$−$C_{ring}$	1.41	1.44	1.427	1.434(1)
	$r$$C_{ring}$−$C_{tBu}$	1.50	1.52	1.520	1.518(2)
	av $r$$C_{tBu}$−$C_{Me}$	1.53	1.54	1.538	1.538(2)
	av rC−H_{ring}		1.08	1.083	1.105(3)
	av rC−H_{Me}		1.11	1.096	1.118(3)
	α	180.0	177.7/179.0	178.5	180.0
	β	0.7	2.5/1.8	0.6	0.0
	γ	6.1	7.0/5.2	6.7	5.5

[a] See text for model description. Abbreviations used: r = bond distance/Å, ∠ = angle/deg, av = average, Δ = difference, ^{t}Bu = *tert*-butyl, Me = methyl, X = center of cyclopentadienyl ring. Precise parameter definitions: p_2 = av (rC−C_{ring} + $r$$C_{ring}$−$C_{tBu}$ + $r$$C_{tBu}$−$C_{Me}$); p_3 = av (rC−H_{ring} + $r$$C_{Me}$−H); p_4 = av [rC−C_{ring} − ($r$$C_{ring}$−$C_{tBu}$ + $r$$C_{tBu}$−$C_{Me}$)]; p_5 = av ($r$$C_{ring}$−$C_{tBu}$ − $r$$C_{tBu}$−$C_{Me}$); p_{11} twist preserves overall C_2 symmetry of molecule (a value of zero means the two ^{t}Bu are coincidental); p_{12} is the ^{t}Bu twist [i.e., dihedral ∠C_{Me}−C−C−Fe, with a value of zero indicating the branch marked * in Figure 1a is coincidental with the perpendicular Fe−Cp distance] and preserves local C_3 symmetry of the ^{t}Bu groups; p_{13} is the Me twist, a value of zero indicating rC−H eclipses $r$$C_{ring}$−$C_{tBu}$. [b] Minima are found at ring twist ϕ = ca. 72° and 144°. [c] Theoretical data quoted with uncertainties are SARACEN restraints used in the GED refinement. [d] Estimated standard deviations (esd's) obtained in the least-squares refinement are given in parentheses.

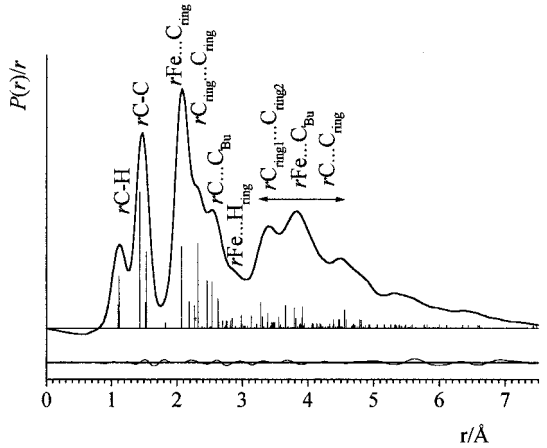

Figure 5. GED experimental and difference (experimental − theoretical) radial distribution curve for **1**. Before Fourier inversion the data were multiplied by $s\cdot\exp[(-0.002s^2)/(Z_{Fe} - f_{Fe})(Z_C - f_C)]$.

of the ring twist parameter p_{11} and, to a lesser extent, the *tert*-butyl twist parameter p_{12}. For the electron diffraction structure, performing an *R*-factor loop, in which the parameter is systematically stepped by given increments, revealed that although an acceptable fit to the experimental data could be obtained when the ring twist parameter p_{11} is ca. 170° ($R_G \approx 0.09$), a better simulation is obtained when p_{11} is ca. 100° ($R_G \approx 0.06$). A Boltzmann analysis of the two minima found by molecular mechanics offers a weighted average ring torsional value of 106°, which is close to that determined experimentally (97.7°). The experimental value for the *tert*-butyl twist parameter p_{12} was in reasonable agreement with those calculated theoretically and found experimentally in the solid phase.

We have also investigated by molecular mechanics 1,1′-derivatives which are more or less sterically demanding than **1**. Rotational profiles for 1,1′-dimethyl, 1,1′-diethyl-, and 1,1′-di-isopropylferrocene (**7**−**9**) are shown in Figure 6. The profile for **7** is almost identical to that of ferrocene, with isoenergetic minima at 0°, 72°, and 144°. Both **7**[14a] and its ferrocenium analogue[17] have essentially 0° eclipsed structures. Increasing the size of the substituent alters little the energies of the 72° and 144° minima, but increases significantly the energy of the 0° eclipsed conformation such that for **9** it now represents a local maximum. Rotational profiles for 1,1′,2,2′- and 1,1′,3,3′-di-*tert*-butylferrocene **10** and **11** are shown in Figure 7. The crystal structure of **10**[18] again has C_{2h} symmetry imposed crystallographically (ϕ = 180°); however, this value clearly lies in the relatively flat region of lowest energy between 144 < 180 > −144°. The ϕ value determined in the solid state for **11**[19] is close to that of the calculated well-defined single minimum in Figure 7.

B. Structure of Isopropylferrocene (2). Crystals suitable for X-ray analysis were grown in a glass capillary by slow cooling to −25 °C, with data collected for structure refinement at −124 °C. The compound crystallizes in the $P\bar{1}$ space group with two molecules per unit cell; molecular conformations are as shown in Figure 8a.

The ring twists (ϕ = 0.2° and 11.9°) and ring substituent twists (H_{iPr}−C−C−Fe = − 47.0° and − 53.0°) for the geometries in the solid state are close to the global energy minimum predicted by molecular mechanics (2.4° and −47.6°, respectively). The complete potential energy surface showed the existence of two main minima at H_{iPr}−C−C−Fe = −50° (enantiomeric equivalent at +50°) and 180° with an energy difference of 1.8 kJ mol^{-1} (Figures 8b and 9). From this energy profile the barrier for isopropyl rotation proceeds via either a low-energy transition state (TS) (4 kJ mol^{-1}; −50 < *TS*1 > 50°) or a higher energy state (7 kJ mol^{-1}; 50 < *TS*2 > 180°). In the solid state the barrier to isopropyl ring rotation has been estimated at 16 kJ mol^{-1}.[15] The inter-ring torsional profile (ϕ) at both energy minima is essentially identical to that of ferrocene with an eclipsed ground-state conformation, indicating insignificant steric interaction between the isopropyl group and the unsubstituted ring. The solid-state barrier for ring rotation is estimated at 33−38 kJ mol^{-1}.[15]

The potential energy surface for **2** was selectively probed using DFT calculations, with starting values for the H_{iPr}−C−C−Fe torsional angle of −90°, 180°, and 0°. Stationary points were located at −50°, 180°, and −3°, which were identified from analytic frequencies as

(17) Tebbe, K.; Buchem, R. *Z. Anorg. Allg. Chem*. **1998**, *624*, 679.
(18) Hughes, R. P.; Kowalski, A. S.; Lompreey, J. R.; Rheingold, A. L. *Organometallics* **1994**, *13*, 2691.
(19) Boese, R.; Blaser, D.; Kuhn, N.; Stubenrauch, S. *Z. Kristallogr*. **1993**, *205*, 282.

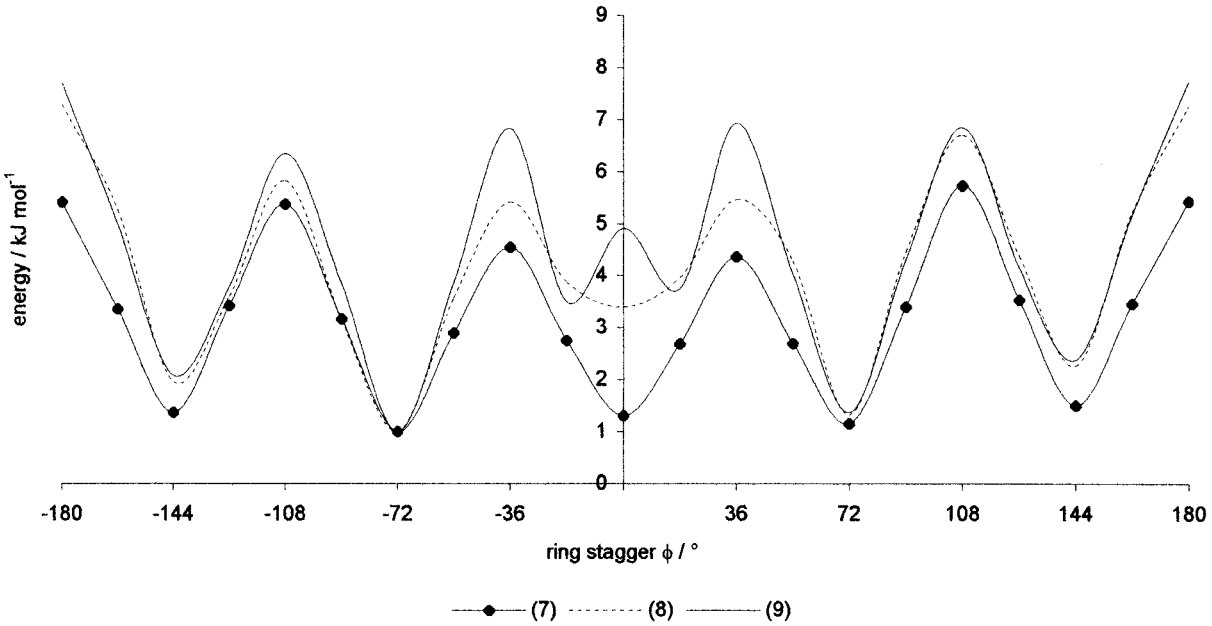

Figure 6. Ring rotational energy profiles for **7**−**9**.

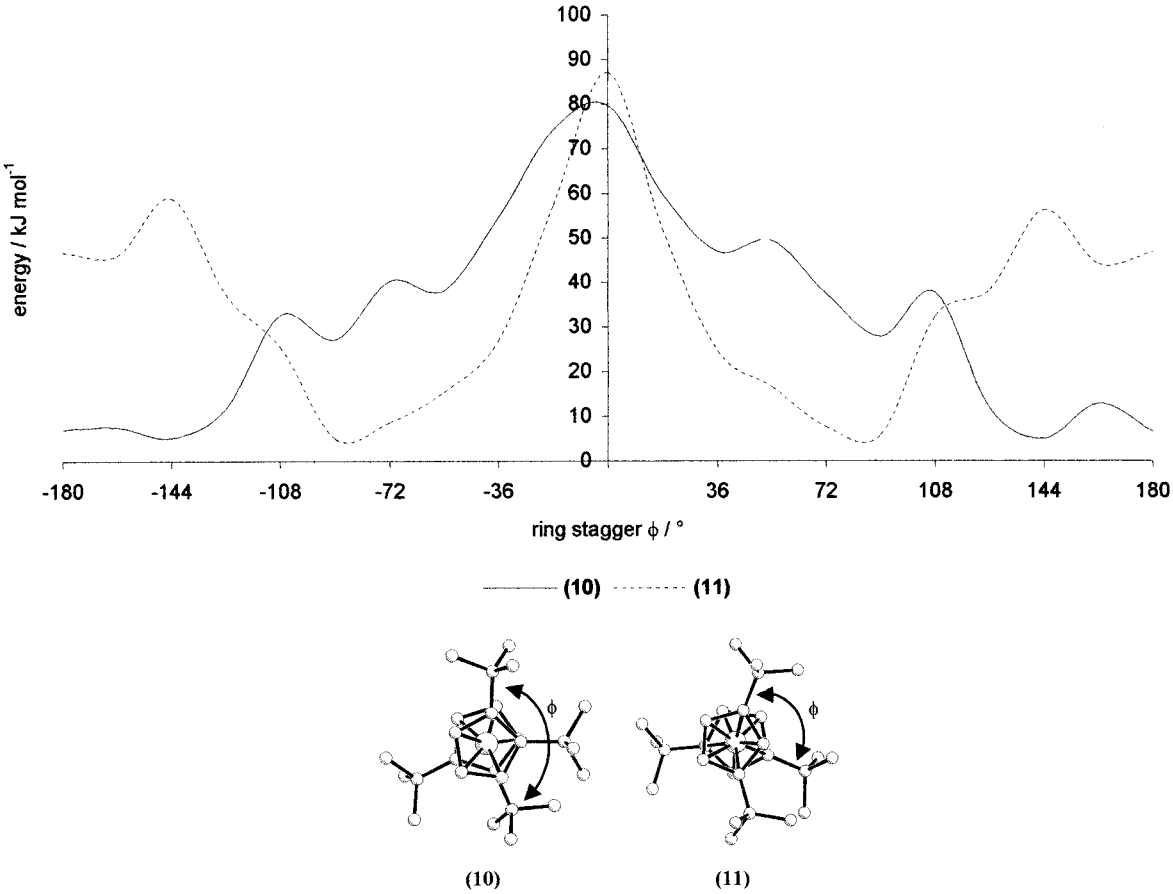

Figure 7. Ring rotational energy profiles for **10** and **11**.

a minimum (global, C_1 symmetry), minimum (local 4.1 kJ mol^{-1}, C_2 symmetry) and a transition state (TS1, 7.9 kJ mol^{-1}, C_1 symmetry), respectively (Figure 8c). All calculated geometries are approximately eclipsed ($\phi \approx 0°$). The DFT calculations therefore support the general shape of the molecular mechanics potential energy surface, but predict higher rotational barriers.

A complete refinement of the gas-phase structure was again achieved using experimental data and values from DFT calculations as input. Two conformers were modeled in the refinement (see Experimental Section), differing only in the value of the ring substituent twist (p_{12}), as the calculated geometries indicate very little structural variation in the other bond distances and angles (Table 5). The conformational weighting was controlled by p_{19}.

The radial distribution curve for **2** (Figure 10) shares many features with that obtained for **1**. The curve

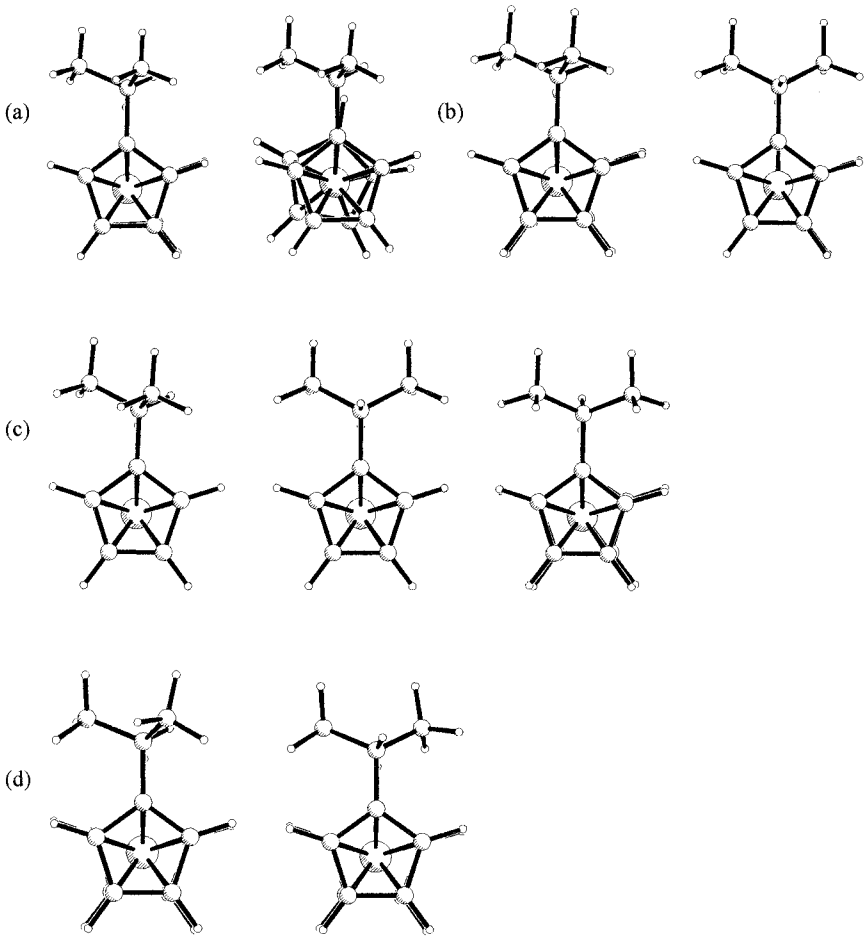

Figure 8. Molecular structures of **2**: (a) X-ray diffraction (two molecules in unit cell), (b) molecular mechanics global and local minima ($H_{ipr}-C-C-Fe = -50°$ and 180°, respectively), (c) DFT global, local minima, and transition state ($H_{ipr}-C-C-Fe = -50°$, 180°, and −3°, respectively), and (d) gas-phase electron diffraction.

comprises four main peaks: the first two define the bonding distances *r*C−H and *r*C−C, the third *r*Fe−X and various C−C−C angles, while the fourth peak directs the overall molecular conformation (i.e., the ring torsional twist p_{11}, ϕ, and the ring substituent twists, p_{12}). Any information regarding the conformational weighting will also be contained in the nonbonding distances under the third and fourth peaks. As with **1**, the key structural features agree with those calculated by DFT. The best fit to the experimental data was also obtained with an eclipsed conformation, in agreement with calculation and the solid-state structure. Several angular parameters, however, refined to values that differ slightly from the calculated geometry. For example, Fe−C−C_{ipr}, p_7, refined to align the isopropyl group with the cyclopentadienyl ring (i.e., $\gamma = 0°$), in contrast to the calculation, which predicted a 4° tilt away from the Fe center. Parameter p_9, Fe−C−H, refined to give the ring hydrogens a tilt of 3° toward the Fe center, compared to just 1° calculated by DFT. Two torsional parameters differed slightly: the methyl group twist refined to ca. 45°, compared to ca. 60° from theory, and the ring substituent twists, p_{12}, also refined to values ca. 10° away from the calculated values.

Varying the weighting of the two conformers had only a minimal effect on the overall simulation of the GED data sets. Introducing the second conformer ($H_{iPr}-C-C-Fe$ = ca. 180°) at 20% of the total gaseous mixture (in line with the DFT energy difference between the global and local minima at the temperature of data collection, taking multiplicity into account) gave no appreciable improvement to the fit obtained modeled on the existence of 100% of the more stable conformer ($H_{iPr}-C-C-Fe$ = ca. −50°). Reducing the conformer ratio to 0.5:0.5 did appear to reduce the quality of the simulation, with the fit-factor R_G increasing by the order of 2%. The weighting is controlled by the relative abundance of the long nonbonding distances concealed under the third and fourth peaks of the radial distribution curve for both conformers; however with few prominent structural features here it proved impossible to determine the exact ratio of the two conformers.

Using our modified force field, we have also investigated the ring−substituent rotational profiles for the eclipsed structures of methyl-, ethyl-, and *tert*-butylferrocene (**12**− **14**), with results shown in Figure 11. Substituting all three hydrogen atoms for methyl groups (i.e., **12** → **14**) results in an increase of ca. 7 kJ mol^{-1} for the 3-fold rotational barrier. All minima have an eclipsed ring configuration. Though experimentally determined structures are not available for **12**−**14**, a recent gas-phase structure[20] of chloroferrocene reveals an eclipsed conformation (also in agreement with molecular mechanics calculation). In the sense that ferrocenes may be regarded as "three-dimensional arenes",

(20) Dronin, B. J.; Dannemiller, J. J.; Kukolich, S. G. *J. Chem. Phys.* **2000**, *112*, 747.

Table 5. Structural Parameters Obtained for 2

	parameter[a]	XRD	MM[b] −50/180°	DFT[c] −50/180/−3°	GED[d]
	independent				
p_1	rFe−C_{ring}	av 2.04	av 2.09	av 2.06	2.058(1)
p_2	av rC−C	1.44	1.46	1.465	1.473(3)
p_3	av rC−H		1.10	1.092	1.088(8)
p_4	ΔrC−C (1)			−0.098	−0.081(6)
p_5	ΔrC−C (2)			−0.024(2)	−0.0238(19)
p_6	ΔrC−H			−0.009(2)	−0.0088(19)
p_7	∠Fe−C−C_{iPr}	126.8/129.1	125.8/130.4	130.5/131.8/128.8	126.2(7)
p_8	∠C_{ring}−C−C_{iPr}	av 111.2	av 111.4/112.7	av 111.5(10)	111.9(7)
p_9	∠Fe−C−H		av 127.7/128.3	av 125.1	123.2(8)
p_{10}	<C−C−H_{Me}		av 111.3/111.5	av 111.0	110.3(9)
$p_{11}(\phi)$	ring twist	0.2/11.9	2.4 /1.0	0.4/0.0/5.8	1.5(8)
p_{12}[e]	∠C_{Me}−C_{iPr}−C−Fe	71.3/65.9	70.6/68.1	69.0/63.3/115.0	77.9(20)/71(7)
	∠H_{iPr}−C_{iPr}−C−Fe	−47.0/−53.0	−47.6/174.6	−50.1/180.0/−3.0	−39.1(20)/172(7)
p_{13}	Me twist		64.2/61.4	av 64.0/62.2/60.2	45(4)
p_{14}	∠C−C−H^{i}Pr		106.8/105.7	av 107.4(10)	107.1(9)
p_{15}	∠C_{Me}−C−C_{Me}	110.8/110.9	110.7/110.2	av 110.6(10)	111.4(9)
p_{16}	conformational weighting				0.8:0.2
	dependent				
	rFe−X	av 1.65	av 1.66	av 1.656	1.659(1)
	av $r$$C_{ring}$−$C_{ring}$	1.42	1.44	1.428	1.432(1)
	$r$$C_{ring}$−$C_{ipr}$	av 1.51	av 1.51	av 1.514	1.501(6)
	av $r$$C_{ipr}$−$C_{Me}$	1.52	1.54	1.532	1.525(6)
	av rC−H_{ring}		1.08	1.088	1.083(8)
	av rC−H_{Me}		1.11	1.097	1.092(8)
	α	av 179.1	179.6/178.4	179.3/178.2/179.8	180.0
	β	av 0.3	0.7/2.0	0.4/0.8/0.8	0.0
	γ	av 2.2	0.1/4.5	3.9/4.8/1.7	0.0

[a] See text for model description. Abbreviations used: r = bond distance/Å, ∠ = angle/deg, av = average, Δ = difference, ^{i}Pr = isopropyl, Me = methyl, X = center of cyclopentadienyl ring. Precise parameter definitions: p_2 = av (rC−C_{ring} + $r$$C_{ring}$−$C_{iPr}$ + $r$$C_{iPr}$−$C_{Me}$); p_3 = av (rC−H_{ring} + $r$$C_{Me}$−H); p_4 = av [rC−C_{ring} − ($r$$C_{ring}$-$C_{iPr}$ + $r$$C_{iPr}$−$C_{Me}$)]; p_5 = av ($r$$C_{ring}$−$C_{iPr}$ − $r$$C_{iPr}$−$C_{Me}$). p_{12} twist preserves the local C_s symmetry of the ^{i}Pr group. Though the dihedral C_{Me}−C−C−Fe is used in the refinement, the dihedral H_{iPr}−C−C−Fe is intuitively easier and is used in discussions in the text. For a value of 0°, the C−H bond eclipses the Fe−X vertical axis. For the Me twist (p_{13}) a value of zero indicates that a C−H bond eclipses $r$$C_{ring}$−$C_{tBu}$. [b] Minima are found at ∠H_{iPr}−C_{iPr}−C−Fe = ca. −50° and 180°. [c] Stationary points are found at ∠H_{iPr}−C_{iPr}−C−Fe = ca. −50°, 180°, and −3° (two minima and transition state, respectively). DFT data quoted with uncertainties are SARACEN restraints used in the GED refinement. [d] Estimated standard deviations (esd's) obtained in the least-squares refinement are given in parentheses.

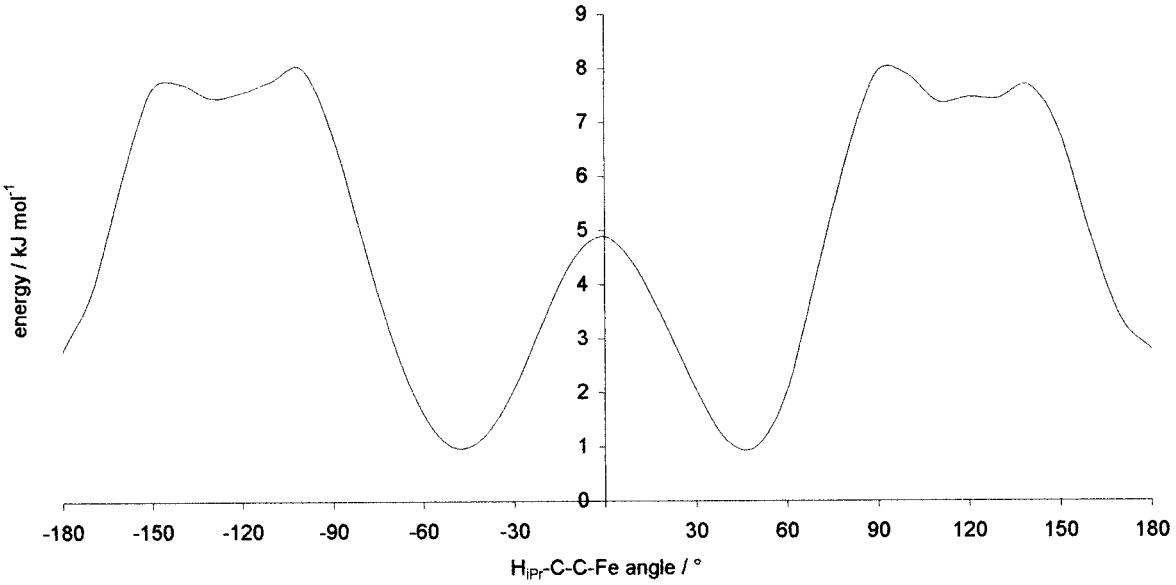

Figure 9. Substituent rotational energy profile for **2**.

it may be noted that the gas-phase structures of ethylbenzene and isopropylbenzene have methyl and hydrogen perpendicular and parallel to the ring plane, respectively,[21a,b] in contrast to **2** and **13**. The global minima for **2** and **13** are essentially the same in terms of substituent orientation toward the more stereodemanding *endo* ring face.

Conclusion

We have demonstrated that a combination of X-ray crystallography, electron diffraction, and DFT calcula-

(21) (a) Schaffer, T.; Sebastian, R.; Penner, G. H. *Can J. Chem.* **1988**, *66*, 1495. (b) Schaffer, T.; Sebastian, R.; Penner, G. H. *Can J. Chem.* **1987**, *65*, 873.

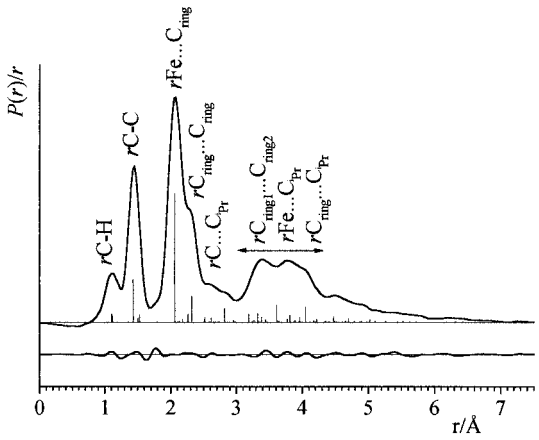

Figure 10. GED experimental and difference (experimental − theoretical) radial distribution curve for **2**. Before Fourier inversion the data were multiplied by $s \cdot \exp[(-0.002s^2)/(Z_{Fe} - f_{Fe})(Z_C - f_C)]$.

tion may be used successfully to analyze the molecular structures of alkylferrocenes. These results have been used as an aid in the development of a molecular mechanics force field which may be generally applied to such derivatives. Future reports will extend this approach to ferrocenes containing unsaturated and heteroatom substituents.

Experimental Section

1. Synthesis of 1,1′-Di-*tert*-butylferrocene (1). A regioisomeric mixture of *tert*-butylcyclopentadiene[22] [^{1}H NMR ($CDCl_3$, 300 MHz) 1.11 (s, 9H, ^{t}Bu), 2.87 (m, 2H, CH_2), 5.90−6.55 (m, 3H, CH=C)] (3.34 g, 27 mmol) was dissolved in dry tetrahydrofuran and cooled to 0 °C under argon. A solution of ^{n}BuLi in hexane (15.4 mL of a 1.6 M solution, 25 mmol) was added dropwise, and the solution was stirred for a further 30 min. In a separate apparatus, anhydrous $FeCl_2$ (1.91 g, 15 mmol) was suspended in dry tetrahydrofuran (60 mL) and cooled to −78 °C. The solution of $LiC_5H_4{}^tBu$ was added slowly by syringe. After warming to room temperature and stirring for 12 h, the solvent was removed and the residue was extracted with 40−60 petroleum ether (3 × 50 mL). After removal of solvent, the product was purified by chromatography (15% deactivated alumina, 40−60 petroleum ether) to give **1** as a viscous orange liquid, which solidified just below room temperature [2.45 g, 54%; ^{1}H NMR ($CDCl_3$, 300 MHz) 1.15 (s, 9H, ^{t}Bu) 3.94, 4.00 (t, 8H, 2 C_5H_4, $J_{2-3/4-5} = J_{2-4/3-5} = 1.8$ Hz); ^{13}C NMR ($CDCl_3$, 75 MHz) 30.4 (CMe_3), 31.4 (CMe_3), 66.0, 68.2 ($C_{2,3}$), 103.4 (C_1)]. Samples for structural work were distilled by Kugelrohr (35−40 °C/0.3 mmHg).

2. Synthesis of Isopropylferrocene (2). $LiAlH_4$ (0.76 g, 20 mmol) was added as a solid to a solution of 2-ferrocenylpropan-2-ol (4.18 g, 17 mmol)[23] in dry ether (40 mL) cooled to 0 °C, followed by dropwise addition of a solution of freshly sublimed $AlCl_3$ (2.67 g, 20 mmol) in dry ether (20 mL). After warming to room temperature and stirring for 1 h, water (50 mL) was added. The aqueous layer was extracted with ether, and the combined ether layers were washed with water. After drying with $MgSO_4$ and evaporation of solvent, the residue was purified by chromatography (alumina, 40−60 petroleum ether) to give **2** as an orange liquid [1.89 g, 48%; ^{1}H NMR ($CDCl_3$, 300 MHz) 1.11 (d, 6H, $CHMe_2$, J = 7.0 Hz), 2.53 (sept, 1H, $CHMe_2$), 3.99 (br s, 4H, C_5H_4), 4.06 (s, 5H, C_5H_5); ^{13}C ($CDCl_3$, 75 MHz) 23.6, 27.5 ($CHMe_2$), 96.9, 66.1, 66.8 (all substituted Cp), 68.2 (unsubstituted Cp)]. Samples for structural work were distilled by Kugelrohr (25−30 °C/0.3 mmHg).

3. Computational Work. All DFT calculations were performed at the DZP/B3PW91 level on a DEC Alpha 1000A workstation using the GAUSSIAN98 code[24] (basis set: 6-31G* for carbon and hydrogen, Wachters + f for iron[25a,b]). Minima were identified by the calculation of analytic second derivative force constants (all positive) at the same level. Cartesian force constants obtained from the vibrational frequency calculations were then used in the construction of scaled harmonic force fields using the ASYM40 program.[26] These force fields were then used to provide estimates of vibration (u) for use in the GED refinements.

HyperChem 5.11 Suite was used on a standard 500 MHz PC for molecular mechanics calculations. Structures were optimized using the MM+ force field (based on Allinger's MM2-(91)), supplemented by the parameters in Table 6.

Optimizations were performed in vacuo, using a root-mean-squared gradient of 0.1 kcal Å^{-1} mol^{-1} as convergence criterion (increased to 0.15 kcal Å^{-1} mol^{-1} for 1,1′-, 1,1′,2,2′-, and 1,1′,3,3′- *tert*-butylferrocenes).

4. Gas-Phase Electron Diffraction. Electron scattering intensities were recorded on Kodak Electron Image photographic plates using the Edinburgh GED apparatus[27] operating at 40 kV. For both **1** and **2** data were recorded at two camera distances, with multiple plates exposed and averaged at each distance. The photographic intensities were then measured using a computer-controlled PDS microdensitometer employing a 200 μm pixel size at the Royal Greenwich Observatory, Cambridge.[28] The sample and nozzle temperatures were maintained at approximately 450 K during the exposure period. Standard programs were used for the data reduction[29] with the scattering factors of Ross et al.[30] The weighting points needed to set up the off-diagonal weight matrixes used in the least-squares refinements are listed in Table 7, together with other experimental parameters.

The GED model for **1** was assumed to have overall C_2 symmetry, in line with the DFT calculations. Each of the two Cp rings was assumed to have local C_{5v} symmetry, with the iron atom lying on the C_5 axis; this assumption meant that a single Fe−C distance was required. The two C_5 axes were chosen to coincide, so that the rings became parallel, and were allowed only to rotate relative to one another. The two rings will not tilt relative to each other if the two *tert*-butyl groups are staggered as predicted ab initio. Each methyl group was

(22) Riemsschneider, R.; Reisch, A.; Horak, H. *Monatsh. Chem.* **1960**, *91*, 805.
(23) Benkeser, R. A.; Bach, J. L. *J. Am. Chem. Soc.* **1964**, *86*, 890.
(24) Frisch, M. J.; Trucks, G. W.; Schlegel, H. B.; Scuseria, G. E.; Robb, M. A.; Cheeseman, J. R.; Zakrzewski, V. G.; Montgomery, J. A., Jr.; Stratmann, R. E.; Burant, J. C.; Dapprich, S.; Millam, J. M.; Daniels, A. D.; Kudin, K. N.; Strain, M. C.; Farkas, O.; Tomasi, J.; Barone, V.; Cossi, M.; Cammi, R.; Mennucci, B.; Pomelli, C.; Adamo, C.; Clifford, S.; Ochterski, J.; Petersson, G. A.; Ayala, P. Y.; Cui, Q.; Morokuma, K.; Malick, D. K.; Rabuck, A. D.; Raghavachari, K.; Foresman, J. B.; Cioslowski, J.; Ortiz, J. V.; Stefanov, B. B.; Liu, G.; Liashenko, A.; Piskorz, P.; Komaromi, I.; Gomperts, R.; Martin, R. L.; Fox, D. J.; Keith, T.; Al-Laham, M. A.; Peng, C. Y.; Nanayakkara, A.; Gonzalez, C.; Challacombe, M.; Gill, P. M. W.; Johnson, B. G.; Chen, W.; Wong, M. W.; Andres, J. L.; Head-Gordon, M.; Replogle, E. S.; Pople, J. A. *Gaussian 98*, revision A.7; Gaussian, Inc.: Pittsburgh, PA, 1998.
(25) (a) Wachters, A. J. H. *J. Chem. Phys.* **1970**, *52*, 1033. (b) Bauschlicher, C. W.; Langhoff, S. R.; Barnes, J. A. *J. Chem. Phys.* **1989**, *91*, 2399.
(26) ASYM40 version 3.0, update of ASYM20; Hedberg, L.; Mills, I. M. *J. Mol. Spectrosc.* **1993**, *160*, 117.
(27) Huntley, C. M.; Laurenson, G. S.; Rankin, D. W. H. *J. Chem. Soc., Dalton Trans.* **1980**, 954.
(28) Lewis, J. R.; Brain, P. T.; Rankin, D. W. H. *Spectrum* **1997**, *15*, 7.
(29) Cradock, S.; Koprowski, J.; Rankin, D. W. H. *J. Mol. Struct.* **1981**, *77*, 113.
(30) Ross, W.; Fink, M.; Hilderbrandt, R. *International Tables for Crystallography*; Wilson, A. J. C., Ed.; Kluwer Academic Publishers: Dordrecht, 1992; Vol. C, p 245.
(31) Sheldrick, G. M. *Shelxtl*; Bruker Analytical X-ray Systems: Madison, WI, 1995.

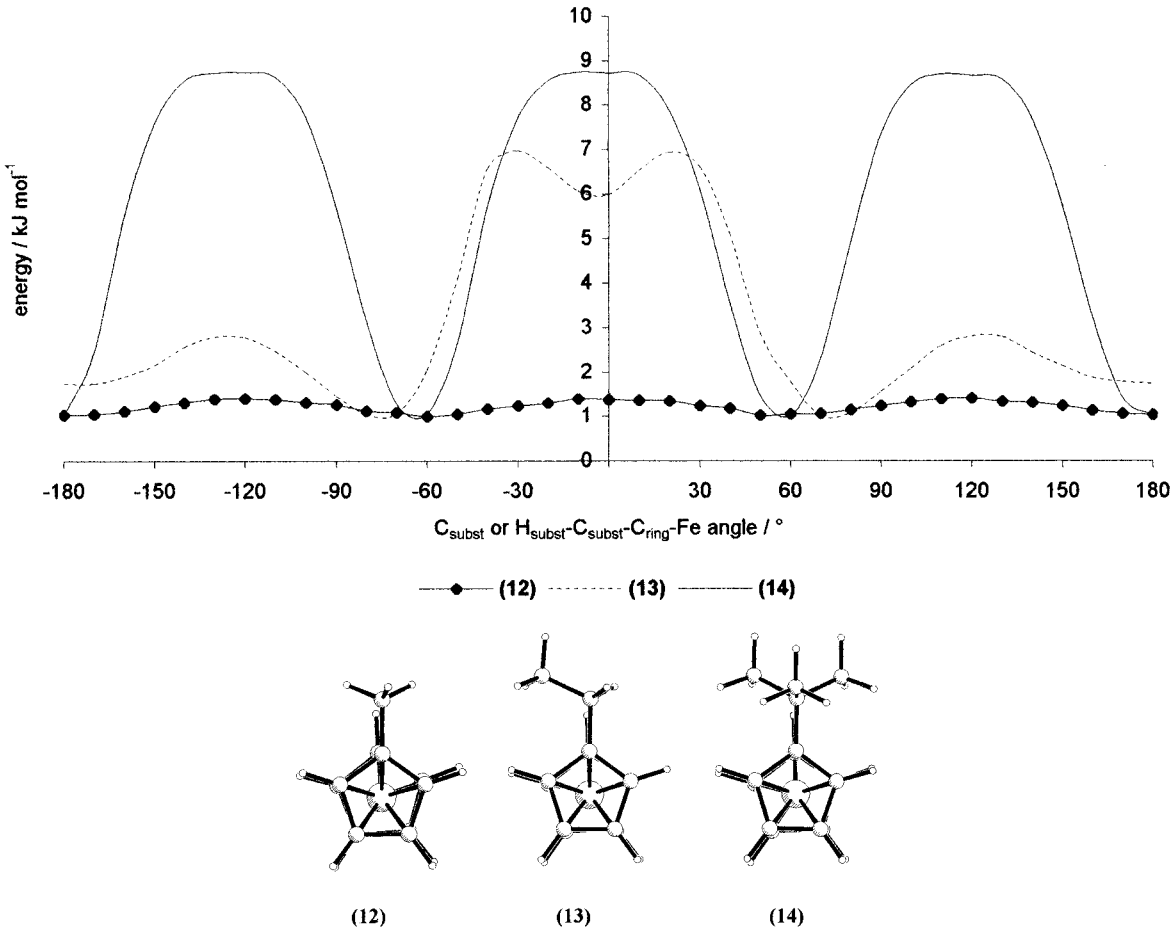

Figure 11. Substituent rotational energy profiles for **12**−**14**.

Table 6. Additional MM Parameters

	mass/g mol^{-1}	description
Cfc	12.000	carbon (ferrocene ring)[a]
Fe	55.847	iron (ferrocene)
LP1	0.001	dummy atom
	Nonbonded	
	R^* (radius)/Å	ϵ (well depth)/kcal mol^{-1}
Fe	2.200	0.020
LP1	0.001	0.001
	Stretching	
	force constant/ mdyn Å^{-1}	equilibrium value/Å
Fe−LP1	50.000	1.630
Cfc−Cfc	8.065	1.420
Cfc−H	4.600	1.080
Cfc−C4	4.400	1.497
	Bending	
	force constant/ mdyn Å rad^{-2}	equilibrium value/°
LP1−Fe−LP1	0.750	180.00
Cfc−Cfc−Cfc	0.430	108.00
Cfc−Cfc−H	0.360	126.00
Cfc−Cfc−C4	0.550	126.00

[a] New atom type Cfc corresponds to type Ca (aromatic carbon), with modifications to reproduce the ferrocene geometry. Only modified parameters are listed.

assumed to have local C_{3v} symmetry, and the ^{t}Bu groups were assumed to possess overall C_3 symmetry. Three different C−C bond lengths were allowed for in the molecule: (a) the internal C−C bonds of the Cp ligand, (b) the bond from the ring carbon to the central carbon of the ^{t}Bu group, and (c) the distance of the methyl carbons to the central carbon of the ^{t}Bu group. Two different C−H bonds were modeled: those belonging to the Cp ring and those of the methyl groups. The hydrogen atoms attached to the Cp ring were assumed to lie in the plane of the ring. In total, 13 structural parameters are required to describe this model fully (Table 4 and Figure 1). Note that to reduce the correlation effects a number of parameters have been defined as average and difference pairs; this is standard practice in GED work. The model for **2** was essentially identical to that for **1**, with changes made relating only to the different ring substituent isopropyl, which was assumed to possess local C_s symmetry. The definition of parameter p_{11} (the ring twist) was changed slightly to represent the degree of staggering between the two rings, instead of formally representing the angle between the two ^{t}Bu substituents as in the previous model. Parameter p_{12} was redefined to represent the isopropyl group torsion. Two additional geometric parameters were then required: p_{14}, which describes the C−C−H_{iPr} angle, and p_{15} describing the C−C−C angle between the two methyl groups on the isopropyl substituent. A full description of the parameters used is given in Table 5 and Figure 1.

The presence of large numbers of similar interatomic distances and of some parameters involving hydrogen (a poor scatterer of electrons) prevented complete structure solutions for both compounds using only experimental data. Information obtained from calculation has therefore been included to allow complete structural determinations using the SARACEN method.[16] The essential feature of SARACEN is that information calculated ab initio is introduced into the refinement procedure as additional observations (or restraints), the weight of the observation being assigned according to the level of convergence achieved in a series of graded ab initio calculations. Adopting the SARACEN method in this work made it

Table 7. GED Data Analysis Parameters

compound	camera distance/mm	weighting functions /nm^{-1} Δs	s_{min}	sw_1	sw_2	s_{max}	correlation parameter	scale factor, k^a	electron wavelength^b/pm
1	252.33	0.2	2.0	4.0	13.0	15.0	0.2845	0.696(7)	0.06016
	91.62	0.4	12.0	14.0	30.4	35.6	0.3954	0.519(22)	0.06016
2	252.33	0.2	2.0	4.0	13.0	15.2	0.4571	0.766(10)	0.06016
	91.56	0.4	8.0	10.0	30.4	35.6	0.3628	0.501(13)	0.06016

Table 8. X-ray Crystallography

	1	2
formula	$C_{18}H_{26}Fe$	$C_{13}H_{16}Fe$
cryst syst	triclinic	triclinic
a/Å	6.0085(15)	7.883(8)
b/Å	7.9718(17)	10.611(9)
c/Å	8.059(2)	13.230(10)
α/deg	88.744(15)	90.85(9)
β/deg	88.079(16)	92.20(8)
γ/deg	78.50(2)	90.74(7)
T/K	120	150(2)
space group	$P\bar{1}$	$P\bar{1}$
μ/mm^{-1}	0.982	1.320
Z	1	4
no. of measd reflns	1337	4512
no. of ind reflns	1337	3694
R_1	0.0651	0.0551
wR_2	0.1530	0.1378
$D_{max, min}$/e Å^{-3}	0.90, −0.76	0.55, −0.71

possible to refine the values of all structural parameters. Final R_G factors for refinement of **1** (which required just two restraints, see Table 4) and **2** (requiring five restraints, see Table 5) were 0.06 and 0.08, respectively, indicating that the data are of good quality and that a good fit between model and experiment has been obtained.

5. X-ray Crystallography. Both **1** and **2** are liquids under ambient conditions, and crystals were obtained by slowly cooling a sample of the material through its melting point while held in a 0.3 mm o.d. capillary mounted on a Stoë Stadi-4 diffractometer equipped with an Oxford Cryosystems low-temperature device. Data were collected in the range $5° < 2\theta < 50°$ with Mo Kα radiation at 120 K (**1**) and 150 K (**2**) (Table 8). The structure of **1** was solved by placing an Fe atom at the origin, while **2** was solved by direct methods. Both structures were refined against F^2 with H atoms in idealized positions and anisotropic displacement parameters on carbon and iron (Shelxtl).[31] A difference map calculated after routine refinement of **1** revealed a prominent difference map peak of 1.6 e Å^{-3} at (00$^1/_2$). This may indicate a small amount of positional disorder in the structure, and it was modeled by simply refining separate scale factors for the l = odd and even data. The cell dimensions of **1** are not very far from being metrically monoclinic; a 2-fold axis about **c** was incorporated into the model, but led to no improvement, so it was discarded. A search for twinning via a supercell was performed but did not suggest any plausible twin laws that might explain the mismatch between the scale factors of the l = odd and even data. The extra scale factor is therefore merely a fitting factor, with no identified physical significance. Its use has no significant effect on refined parameters. Supplemental crystallographic data have been deposited at the Cambridge Crystallographic Data Centre.

Acknowledgment. We thank the UK Computational Chemistry Facility (Department of Chemistry, Kings College London, Strand, London WC2R 2LS) for computing time on Columbus (D.W.H.R.), EPSRC for financial support of the Edinburgh Electron Diffraction Service (Grant GR/K44411) (D.W.H.R) and for use of the Daresbury Chemical Database Service (J.A.S.H.), and the Society of Chemical Industry for a Messel Scholarship (N.F.). The iron basis set was obtained from the Extensible Computational Chemistry Environment Basis Set Database (Version 1.0) as developed and distributed by the Molecular Science Computing Facility, Environmental and Molecular Sciences Laboratory, Pacific Northwest Laboratory, P.O. Box 999, Richland, WA 99352. The Pacific Northwest Laboratory is a multiprogram laboratory operated by the Batelle Memorial Institute and funded by the U.S. Department of Energy under Contract DE-AC06-76RLO 1830.

Supporting Information Available: Molecular scattering intensities and final correlation matrixes for the GED work, tables of crystal data and structure refinement details, atomic coordinates, bond lengths and angles, and anisotropic displacement parameters and full sets of Cartesian coordinates (pdb format) for the structures calculated by DFT and GED are available as electronic Supporting Information. This information is available free of charge via the Internet at http://pubs.acs.org.

OM001012W